Anodic Oxidation of Galena (PbS) Studied FTIR-Spectroelectrochemically

I. V. Chernyshova†

St. Petersburg State Technical University, Polytechnicheskaya 29, 195251 St. Petersburg, Russia

Received: March 19, 2001; In Final Form: June 9, 2001

The attenuated total reflection/FTIR spectra of the (100) galena/electrolyte interface were measured in situ for the first time in nitrogen-saturated borate buffers (pH 9.2) of two concentrations in the potential region of −0.5 to +0.7 V (SHE), simultaneously with the voltammograms. The experiments were conducted on the electrode previously reduced at −0.5 V and the nonreduced electrode as well. Not only vibrational bands but also monotonic absorption of free carriers was analyzed. It was concluded that at the first step galena is oxidized by the reaction $PbS + 2xh^+ \Rightarrow Pb_{1-x}S + xPb^{2+}$, which is followed by the reaction $PbS + 2h^+ \Rightarrow Pb^{2+} + S°$. $Pb(OH)_2$ is formed by the precipitation mechanism. The $Pb(OH)_2$ yield of galena oxidation increases as either the buffer concentration or the time of the galena reduction is increased, which was explained by an increase in the potential drop in the Helmholtz layer. When a more positive bias potential is applied, lead sulfite and thiosulfate are formed by the reactions $PbS + 3H_2O \Rightarrow PbSO_3 + 6H^+ + 6e$ and $PbS + S° + 3H_2O \Rightarrow PbS_2O_3 + 6H^+ + 8e$, respectively. These processes were correlated with the galena floatability.

Introduction

Galena (natural PbS) is a semiconductor with a band gap of about 0.4 eV, mainly of n-type conductivity.[1] This mineral is a major industrial source of lead and toxic contamination of water, causing serious environmental problems. Synthetic lead sulfide is used in IR detectors and has been regarded as a promising material for solar energy conversion. For these reasons, as noticed,[2] "surface oxidation of lead sulfide (galena) has been the object of countless studies" (for reviews, see refs 2−4). It is generally now accepted that the galena oxidation in aqueous media can be considered as electrochemical corrosion with oxygen reduction as the cathodic process, but there still is no agreement in regard to the mechanism of the anodic process. In the voltammograms measured in 0.05 M borate (pH 9.2), the anodic current is preceded by a prepeak at +0.15[5,6] or +0.20[7,8] V (SHE). On the other hand, the potential dependence of collectorless flotation of galena in an oxygen-free solution of pH 8 has the maximum at ca. +0.25 V,[9] while the galena ground in a reducing environment is floated in 0.01 M bicarbonate buffer of pH 9.2 at +0.45 V.[10] The oxidation state of the sulfide affects its interaction with collectors (selectively adsorbed surfactants), specifically alkyl xanthate.[11] To interpret the electrochemical and flotation regularities, the following reactions have been suggested in the literature.

The initial oxidation stage (the prepeak in the voltammograms) has been interpreted as

(I) formation of a metastable sulfur-rich sulfide underlayer, yielding a monolayer of PbOH[12] or $Pb(OH)_2$ in alkaline solutions[13−16]

$$PbS + 2H_2O + 2xh^+ \Rightarrow Pb_{1-x}S + xPb(OH)_2 \quad (1a)$$

or injecting lead cation (incongruent dissolution) into acidic solution[1,17]

$$PbS + 2xh^+ \Rightarrow Pb_{1-x}S + xPb^{2+} \quad (1b)$$

where h^+ stands for hole.

(II) At pH 7−10, direct formation of elemental sulfur and a monolayer of PbO,[7] $Pb(OH)_2$[18−21]

$$PbS + 2H_2O + 2h^+ \Rightarrow Pb(OH)_2 + S° + 2H^+ \ (E° = +0.757 \text{ V}) \quad (2)$$

or lead borate[5,22] (in borate buffer).

(III) Congruent dissolution−oxidation[2,23−27]

$$PbS \Rightarrow Pb^{2+} + S^{2-} \quad (3)$$

which is followed by hydrolysis of the anion and cation and anodic oxidation of hydrolyzed sulfur to elemental sulfur ($HS^- \Rightarrow S° + H^+ + 2e$ at pH 9.2).[25]

Decomposition at pH 7−10 in the higher overpotential region, in which galena behaves as a quasimetal, has been interpreted as reaction 2,[19,20,28,29] but yielding a bulk oxidation layer with $(OH)_2$ and Pb vacancies [20,21] as charge carriers. Instead of $Pb(OH)_2$, lead carbonate can form.[30] As an alternative, lead hydroxide can appear simultaneously with

(IV) lead thiosulfate[29]

$$2PbS + 5H_2O \Rightarrow PbS_2O_3 + Pb(OH)_2 + 8H^+ + 8e \ (E° = +0.505 \text{ V}) \quad (4)$$

or

(V) anions of thiosulfate[7,22,28,31] or more thermodynamically stable sulfate[23]

$$2PbS + 7H_2O \Rightarrow 2Pb(OH)_2 + S_2O_3^{2-} + 10H^+ + 8e \ (E° = +0.611 \text{ V}) \quad (5a)$$

$$2PbS + 2CO_3^{2-} + 3H_2O \Rightarrow 2PbCO_3 + S_2O_3^{2-} + 6H^+ + 8e \ (E° = +0.218 \text{ V}) \quad (5b)$$

$$2S° + 3H_2O \Rightarrow S_2O_3^{2-} + 6H^+ + 6e \ (E° = +0.310 \text{ V}) \quad (5c)$$

(reactions for sulfate are similar to reactions 5a and 5b).

† E-mail: Irina.Chernyschova@pobox.spbu.ru. Fax: +7 (812) 428-5712.

10.1021/jp0110253 CCC: $20.00
Published on Web 08/07/2001

Reaction 3 has been suggested on the basis of the combined atomic force microscopy (AFM) and X-ray photoelectron spectroscopy (XPS) data[25] obtained at pH 4.9, but it is unclear whether it is valid at alkaline pH's. Reactions 2, 4, and 5 are consistent with data provided by classical electrochemical methods[1,5−8,12,18−21,28,29] and measurements of the surface photovoltage,[5,6] the flotation response,[9,10] and the solution composition.[26,27] However, implications of them will always be questioned until confirmed by an in situ spectroscopic method, which is common for all indirect methods. Reactions 1 have been put forward[13,14] to explain lead enrichment of slightly oxidized galena surfaces observed by XPS.[3,13−16] However, despite numerous attempts,[2,13,14,32,33] sulfur in the oxidation state higher than −2 has not been firmly detected so far on the galena slightly oxidized at neutral to alkaline pH's. This discrepancy can be attributed to intrinsic instability of the sulfur-rich layer relaxing at the open circuit potential (OCP)[16] or to intrinsic instability of sulfoxy species in the presence of atmospheric CO_2 and in UHV.[32] Moreover, the natural presence of surface contamination has been shown[2] to inhibit oxidation at OCP and interfere with analysis of the XPS spectra.

The absence of a consensus with regard to the mechanisms of galena anodic oxidation can be explained, in our viewpoint, in addition to the complex surface chemistry and the instability of the surface films on semiconducting sulfides, by the fact that the problem has not been studied in situ spectroscopically yet. The exception is Raman scattering work, [34] which, however, revealed[35] that the method is insensitive to the surface film formed at the initial stage of the galena oxidation (elemental sulfur was detected only at +0.37 V to +1.24 V).

Thus, the present state of knowledge about galena anodic oxidation in aqueous solution needs application in situ of a spectroscopic method capable of detecting the products of reactions 1−5 with sensitivity on the order of fractions of a monolayer. In our viewpoint, this method is FTIR spectroscopy, which is widely used in electrochemistry due to a large body of information provided, simplicity of the application in situ, and availability.[36] However, application of FTIR spectroscopy to the field of electrochemistry of single-crystal semiconducting electrodes has so far been restricted to microelectronics-related semiconductors (e.g., Si,[37] GaAs,[38,39] and, as a model, Ge[40,41]), from which an internal reflection element (IRE) can be made. However, this technique is inapplicable to natural minerals,[42] while another convenient attenuated total reflection (ATR) technique[43] uses artificial minerals whose adsorption characteristics differ from those of natural prototypes.[44] As discussed,[11] the ATR technique using a glued mineral plate[42] not only overcomes this problem, but is characterized by a better optical performance as compared to the particle-electrode[45] and external reflection[46] techniques previously used for probing in situ the sulfide electrode surface.

The goal of this work was to study in situ using the ATR/FTIR technique[42] the anodic processes on a galena electrode in N_2-saturated borate buffer (pH 9.2).

Experimental Section

In situ ATR/FTIR spectra of the galena/solution interface were measured in the spectroelectrochemical cell described in detail elsewhere.[42] Classical electrochemical equipment (potentiostat PI-50-1 and programmer PR-8, Russia) was employed in three-electrode configuration. The counter electrode was a Pt wire. The potentials were measured against a saturated potassium chloride electrode connected via a Luggin capillary to the cell, while all potentials reported here were converted to the standard hydrogen electrode (SHE). The current−potential ($I-V$) dependencies were measured with an $X-Y$ recorder.

The working electrode was prepared from single-crystal galena, whose minor elements (Ag (3000 ppm), Sb (1200 ppm), and Sn (40 ppm)) were determined by mass spectrometry with an INA-3 Leybold AG instrument. A galena plate, which was cut parallel to a (100) crystallographic plane of the crystal, was glued by using a low-melting halcogenide glass to a halcogenide glass hemicylindric IRE. Before each experimental run, the working surface was wet polished successively with 1.0 and 0.3−0.05 mm alumina (Buehler) and washed thoroughly with distilled water. The polished surface is expected[21] to be close to the damaged mineral surface created by grinding in mills before flotation. After that, the "glued plate−IRE" assembly was attached to the cell, the cell was filled with the N_2-saturated buffer, and the electrode potential was changed according to a selected program. The spectrum measured at −0.5 V after the electrode reduction or at the OCP was the reference spectrum for the reduced or nonreduced electrode, respectively. The electrode was kept at each selected potential for 5 min, including 2 min for acquisition of a 200-scan spectrum. The single-beam ATR/FTIR spectra were recorded at 8 cm^{-1} resolution at each step, at an angle of incidence of 37°, with a Perkin-Elmer model 1760 FTIR spectrometer equipped with a Micro ART unit TR-5 and MCT detector, and represented either in reflectivity (R/R_0) or absorbance ($-\log(R/R_0)$) units, where R and R_0 are the spectra at the sample and reference potentials, respectively. No smoothing of the spectra was performed.

Borate buffer solutions were prepared with commercial $Na_2B_4O_7{\cdot}10H_2O$ of analytical grade in bidistilled water. Deaeration was achieved by 1 h of boiling of the buffer with bubbling of high-purity nitrogen through the solution. Nitrogen was bubbled also during the following spectroelectrochemical experiments, which provided mixing.

Results and Discussion

The FTIR-spectroelectrochemical measurements were performed in 0.01 and 0.05 M N_2-saturated borate (pH 9.2) first for the galena electrode, which was previously reduced at a potential of −0.5 V for 1 h to provide the experiment reproducibility and to remove the surface oxidation products.[8,18,21] The current−potential ($I-V$) dependencies, which were measured simultaneously with the spectra, are shown in Figure 1a. The shape of the dependencies resembles that reported in other works,[5−8] including the prepeak at ca. +0.15 and +0.10 V in 0.01 and 0.05 M borate, respectively. The corresponding ATR spectra are shown in Figures 2 and 3. To distinguish the spectrum changes at each step, the spectrum at a marked potential is referenced to the spectrum at the preceding potential.

In the case of 0.01 M borate (Figure 2), neglecting smooth background changes (see below), the anodic oxidation first characterized by weak broad bands at 1360 and 960 cm^{-1} appeared at +0.2 V. An additional narrow band arises at 982 cm^{-1} (marked by an arrow in Figure 2a) at +0.3 V. At more positive potentials, this band is accompanied by a satellite at 1007−1010 cm^{-1}, while the broad band at 960 cm^{-1} splits into components 1220, 1115−1120, and 950 cm^{-1}. Since lead hydroxide, carbonate, and lead polyborates have the principal band at 1360−1440 cm^{-1}, the origin of the band at 1360 cm^{-1} was determined[33] by the XPS method. Boron and carbonate carbon were not detected. On the basis of the Pb 4f, O 1s, S 2s, and S 2p peaks, the surface oxidation product was identified as $Pb(OH)_2$. The comparison with the reference spectra of lead sulfite,[43] lead thiosulfate,[47] and solvated sulfoxy anions (Figure

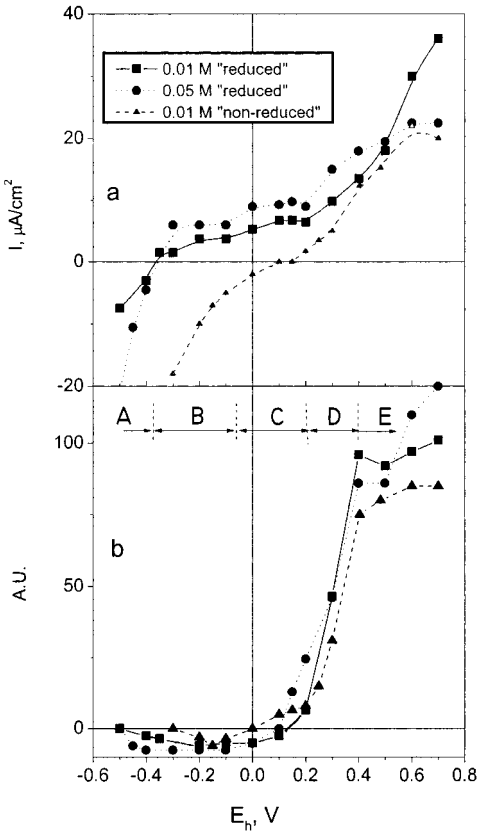

Figure 1. (a) $I-V$ dependencies of a (100) galena electrode in 0.01 M (■ and ▲) and 0.05 M (●) borate buffer (pH 9.2), measured simultaneously with the ATR/FTIR spectra shown in Figures 2, 3, and 6. The electrode was initially reduced at −0.5 V (■ and ●) or nonreduced (▲). (b) Dependence of the smooth background at low wavenumbers on the electrode potential, taken at 800 cm^{-1} in the spectra referred to the spectrum measured at the initial cathodic potential.

4) allows assignment of the band at 960−950 cm^{-1} to the $\nu_{as}(SO_3^{2-})$ mode of bulk $PbSO_3$ and the bands at 1115−1120 and 982 cm^{-1} to, respectively, the $\nu_{as}(SO_3^{2-})$ and $\nu_s(SO_3^{2})$ modes of bulk PbS_2O_3. The pair of bands at 1220 and 1007−1010 cm^{-1} are similar in shape to and increase in concert with the pair of bands of bulk PbS_2O_3. They can be assigned to a less stable crystallographic modification of lead thiosulfate, in which the $S_2O_3^{2-}$ ion coordinates Pb^{2+} by S-bridging.[48] The spectrum of the stable PbS_2O_3 form differs from that of solvated thiosulfate ion only by the downshift of the $\nu_s(SO_3^{2-})$ band by 15−18 cm^{-1}. Therefore, we carried out additional experiments to check the above assignment. The spectrum of the oxidized galena/electrolyte interface was found to be unaffected by stirring the solution. Moreover, when the potential bias from +0.6 to 0 V was applied, the pair of bands at 1220 and 1007−1010 cm^{-1} disappeared first (Figure 5). These results allow one (i) to rule out reactions 5 in which solvated sulfoxy ions form before their precipitation as complexes with lead and (ii) to conclude that the reaction

$$PbS + 3H_2O \rightleftharpoons PbSO_3 + 6H^+ + 6e \qquad (6a)$$

precedes or at least accompanies the formation of PbS_2O_3.

Contrary to the previous case, the ATR spectra exhibit in 0.05 M borate distinct broad bands at 1410, 1090, and 860 cm^{-1} from 0 to +0.2 V (Figure 3a). Being similar but not identical to the spectrum of a borate solution (Figure 4), they can be assigned to physically adsorbed polyborate anions as well as the first monolayer of lead borate in agreement with previous

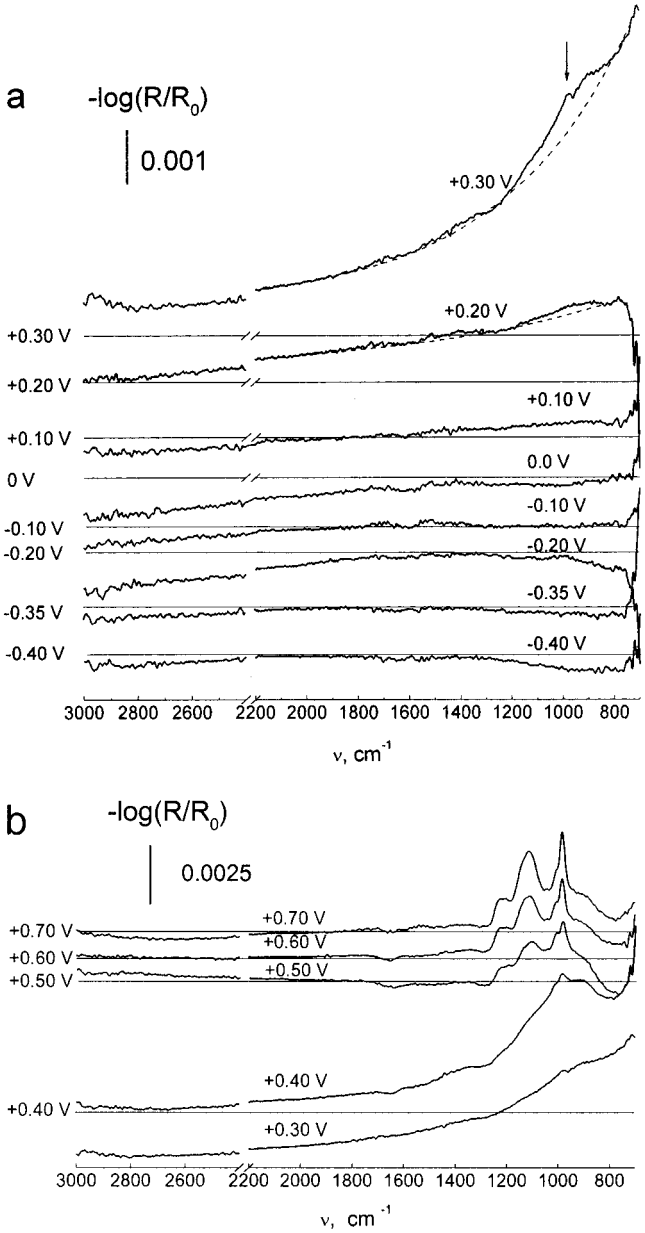

Figure 2. ATR spectra of the (100) galena/solution interface measured during the anodic scan of potential in 0.01 M borate. Before the experiment, the electrode was polarized at −0.5 V for 1 h. The spectrum at a marked potential is referenced to the spectrum at the preceding potential, while the spectrum at −0.4 V is referenced to the spectrum measured at −0.5 V after the reduction. The horizontal lines indicate zero absorption. The dashed lines indicate hole absorption.

impedance[21] and voltammetric[5,22] data, respectively. These bands arise against increasing surface concentration of holes (see below), and bulk lead hydroxide is formed at the next stage. On this basis, we attribute them to physically adsorbed borate species. (This assignment does not eliminate the possibility of hydroxyl adsorption since the δ(OH) band can be overlapped.)

The spectrum at +0.3 V in 0.05 M borate is similar to that in 0.01 M borate (compare Figures 2a and 3a), exhibiting the bands of the lead sulfoxy compounds and the double band at 1360 cm^{-1} of $Pb(OH)_2$. However, the amount of lead hydroxide is significantly higher in the former case. This relationship also holds at higher potentials (compare Figures 2b and 3b), implying that only the reaction for $Pb(OH)_2$ is accelerated by increasing the ionic strength of the indifferent buffer. Thus, formation reactions for the sulfoxy compounds and $Pb(OH)_2$ are different,

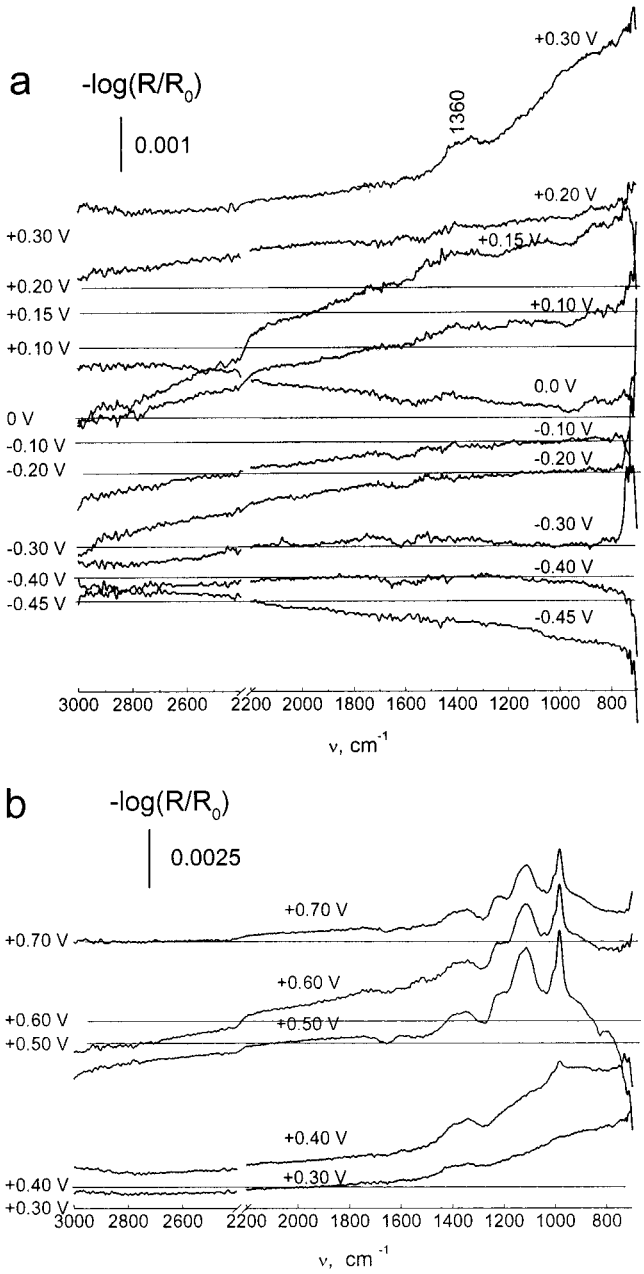

Figure 3. ATR spectra of the (100) galena/solution interface measured during the anodic scan of potential in 0.05 M borate. Before the experiment, the electrode was polarized at −0.5 V for 1 h. The spectrum at a marked potential is referenced to the spectrum at the preceding potential, while the spectrum at −0.45 V is referenced to the spectrum measured at −0.5 V after the reduction. The horizontal lines indicate zero absorption.

and reaction 4a should also be ruled out. The possible reaction of PbS_2O_3 formation without releasing lead cations is

$$PbS + S^\circ + 3H_2O \Rightarrow PbS_2O_3 + 6H^+ + 8e \ (E^\circ = +0.420 \text{ V}) \quad (6b)$$

which flows when elemental (active[49]) sulfur and a PbS unit are in close vicinity to each other. This requirement imposes kinetic limitations on the formation of PbS_2O_3.

Taking into account that the voltammetric curves were obtained in refs 5−7 without previous conditioning of the polished electrode at a reducing potential, we repeated the experiments in 0.01 M borate, but the potential was increased from −0.3 V just after measuring the reference spectrum at the

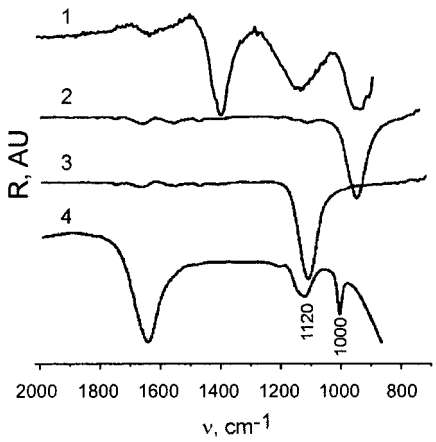

Figure 4. ATR spectra of aqueous solutions of (1) $Na_2B_4O_7 \cdot 10H_2O$, (2) Na_2SO_3, (3) $NaSO_4$, and (4) NaS_2O_3, measured with a Circle accessory.

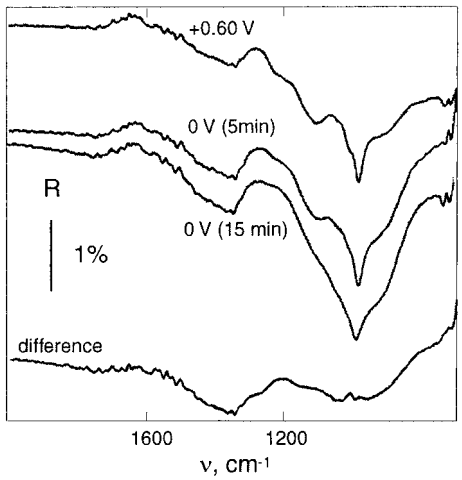

Figure 5. ATR spectra of the (100) galena/solution interface measured at +0.6 V after the anodic scan of potential in 0.01 M borate from −0.5 V and then conditioned for 5 and 15 min at 0 V. The difference spectrum relates to the spectrum taken at +0.6 and 0 V (15 min). Before the experiment, the electrode was polarized at −0.5 V for 1 h.

OCP of +0.163 V. For this electrode (called "nonreduced" below), the prepeak is absent in the $I-V$ curve (Figure 1a). As seen from Figure 6, the spectral changes from −0.3 to +0.2 V present a series of negative complex bands at ca. 1615, 1380, and 1050 cm^{-1}. The band at 1615 cm^{-1} is due to the interfacial water reorganized upon the potential increase. Being undetectable in the case of the reduced galena in 0.01 M (Figure 2a), the bands at 1380 and 1050 cm^{-1} can be ascribed to the oxidation film mainly consisting of lead hydroxide and sulfate, which cover the as-polished galena surface and are slowly reduced at alkaline pH (see also ref 33). At potentials higher than +0.25 V, the spectra are similar to those shown in Figures 2 and 3, except for the practical absence of the 1360 cm^{-1} band of lead hydroxide. This observation confirms that the reactions for $Pb(OH)_2$ and lead sulfoxy salts are different, and testifies that the formation of $Pb(OH)_2$ is suppressed by incomplete reduction of the electrode.

Thus, the $Pb(OH)_2$ yield depends on the indifferent buffer concentration and the surface pretreatment. To arrive at more detailed conclusions, additional information is required, which, as shown below, can be provided by analysis of the low-wavenumber background. Inspecting the spectra shown in Figures 2, 3, and 6, one can notice regularities in the behavior of the smooth background at low and high wavenumbers with

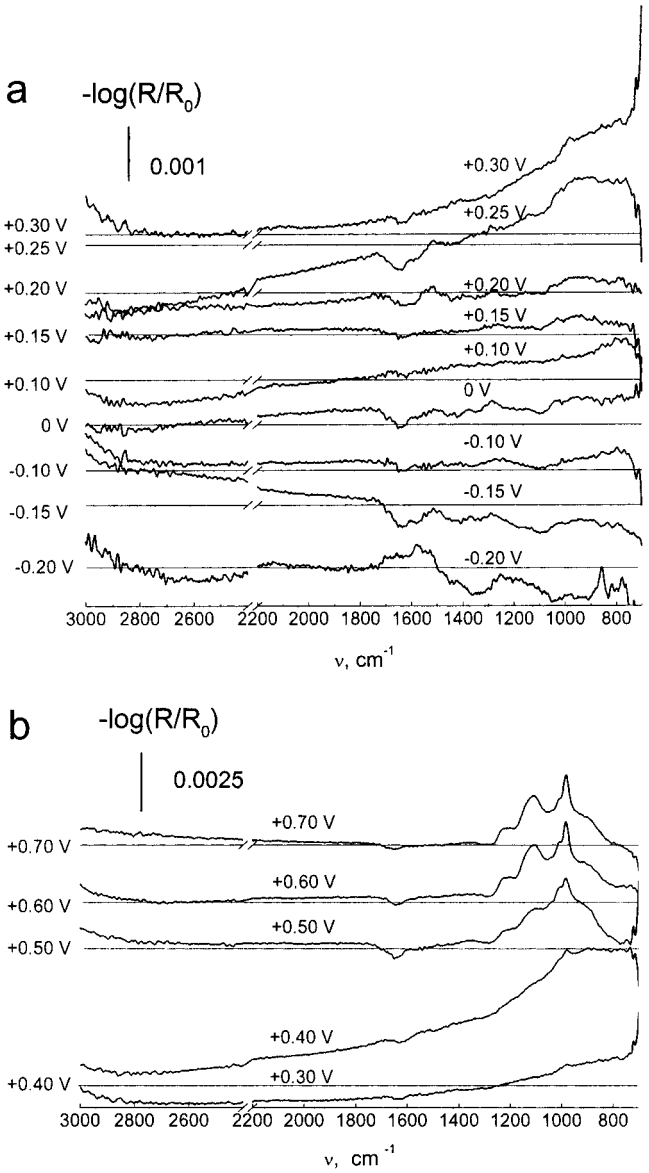

Figure 6. ATR spectra of the (100) galena/solution interface measured during the anodic scan of potential in 0.01 M borate. Before the experiment, the electrode was not reduced. The spectrum at a marked potential is referenced to the spectrum at the preceding potential, while the spectrum at −0.20 V is referenced to the spectrum measured at the initial OCP.

the boundary at ca. 1500 cm^{-1}. The low-wavenumber background is marked by dashed curves in Figure 2a. To follow these changes, the background absorption at 800 cm^{-1} was measured relative to that in the spectrum obtained at −0.5 and −0.3 V for the reduced and nonreduced electrodes, respectively, and plotted as a function of potential in Figure 1b. In the case of the reduced electrodes, the background first somewhat decreases upon anodic polarization, then is constant within a certain interval of potentials, and after that grows exponential-like. This process is essentially slowed from +0.4 V, where the absorption is proportional to the amount of formed $Pb(OH)_2$ and does not correlate with the current density. The described potential regions for 0.05 M borate are labeled in Figure 1b by A, B, C, D, and E. It was found in independent experiments that the low-wavenumber background absorption is reversible and responds to the potential changes without a noticeable time delay. As the time of the reduction at −0.5 V decreases, region B becomes narrower and shifts anodically (not shown), disappearing in the limiting case of the nonreduced electrode (Figure 1b).

By analogy with the ATR spectra of the Si/electrolyte[37] and Ge/electrolyte[40,41] interfaces, we assign the low-wavenumber absorption to free carriers whose concentration in the space charge layer is modulated by the electrode potential. Assuming that 1 h of reduction at −0.5 V produces a galena surface layer of the n-type,[1,5,6,21] one can attribute the decrease in free carrier absorption in region A to subtraction of electrons from the accumulation layer. In region B, free carrier absorption is constant and minimal, as expected for the depletion regime. The onset of region B at −0.30 and −0.4 V in 0.01 and 0.05 M borate, respectively, is somewhat more anodic[39−41,50,51] than the flat band potential, which confirms that the reduced electrode is of n-type conductivity.[1,6] Region C coincides with the prepeaks in the $I-V$ dependencies (Figure 1a). Here, the electrode is in the inversion regime when holes are thermally generated in sufficient concentration to promote the galena decomposition without degeneracy. In agreement with theory,[51] the concentration of holes and, hence, the upward band bending increase as the buffer ionic strength increases, which is balanced by a higher excess of borate anions in the outer Helmholtz plane. As a result, the negative drop of potential in the Helmholtz layer is higher, which provides[52] a higher rate of injection of lead cations into solution. Region D spreads from ca. +0.2 V (the onset of the basic anodic current) to +0.4 V. In this region, anodic decomposition is accelerated since the Fermi level is pinned at the edge of the valence band and the potential drops solely on the solution side of the double layer, i.e., the sulfide behaves like a metal. This explains why hole absorption in region D becomes independent of the electrode pretreatment and the buffer concentration. Finally, in region E, the main surface reaction becomes the formation of the lead sulfoxy compounds by reactions 6a and 6b. The rate of accumulation of holes decreases since the holes captured by sulfur now leave the PbS crystal. In parallel, $Pb(OH)_2$ is still formed, supplying holes.

The fact that holes are generated and accumulated at the interface during the galena decomposition in regions C, D, and E implies the formation of a sulfur-rich layer, which is inconsistent with reaction 3. Since the intensity of the $Pb(OH)_2$ band (Figures 2b, 3b, and 6b) is proportional to the hole absorption in region E (Figure 1b), one can conclude that the formation of $Pb(OH)_2$ implies generation of holes. The reverse is not true. There is no $Pb(OH)_2$ on the nonreduced electrode up to +0.4 V, while the anodic current is significant and holes are generated. On this basis, reactions 1a and 2 are ruled out. Thus, even at alkaline pH's, the initial step of the anodic oxidation of galena can be described by reaction 1b, ignoring hydrolysis of lead cations. The reaction

$$PbS + 2h^+ \rightleftharpoons Pb^{2+} + S^\circ \ (E^\circ = +0.354\ V) \qquad (7)$$

rather than reaction 2 appears to be responsible for the fist stage of bulk oxidation, and as noticed,[9] its onset is close to the flotation edge. Lead hydroxide is formed by precipitation when the solubility product is reached at the interface, which is controlled not only by the pH of the electrolyte but also by the potential drop in the double layer. The release of lead cations during the galena oxidation is also consistent with the observed inhibiting role of Pb^{2+}.[12]

In the case of the nonreduced galena, the flat band potential is somewhat higher than −0.1 V, which suggests high p-type conductivity.[1,6] Therefore, the galena surface at the OCP (+0.163 V) is degenerate by holes, while at −0.3 V it is in the

inversion regime. Since the flat band potential is below the decomposition potential of reaction 1b, the inversion region is at once followed by an accumulation region (Figure 1b). The slowest rate of the anodic reactions 1b and 7 for the nonreduced galena in the 0 to +0.4 V range can be explained by the presence of a nonreduced surface layer which hinders the diffusion of Pb^{2+} ions or changes the double layer structure, resulting in a decrease in the negative potential drop in the Helmholtz layer, by analogy with the passivating role of oxygen in the anodic dissolution of metals.[52]

A question can arise about how the above interpretation correlates with the solubility product, K_{SO}, of lead polyborates and lead hydroxide. From free energy data,[53] which are typically used in the thermodynamic calculations (for example, see refs 8−10, 30, and 54), the value of K_{SO} for $Pb(OH)_2$ is −14.37, while the experimental values reported are, e.g., −19.96,[55] −16.79,[56] −15.90,[57] and −12.17.[58] According to the experimental data,[56] at alkaline pH borate anions interact with lead ions with the formation of lead diborate, $Pb(BO_2)_2$, which is characterized by $K_{SO} = -10.78$. This means that $Pb(BO_2)_2$ is much less stable than $Pb(OH)_2$.

Finally, consider the high-wavenumber background (Figures 2 and 3). For the reduced galenas, it is most pronounced in regions B and C, presenting a down-going slop at $\nu > 1500$ cm^{-1}. The more concentrated the electrolyte, the larger this slope (Figures 2 and 3). For the nonreduced electrode, the slope is upward in the −0.3 to −0.15 V range, absent at −0.10 to 0 V, and then slightly downward. On the basis of the literature data, the high-wavenumber background could be assigned either to metallic lead deposited by the reduction[59] or to the surface states.[60,61] It was found in separate experiments that the slope is downward when the galena potential is decreased from the OPC to −0.5 V and absent when galena is further reduced to −1.2 V. At the following anodic potential bias, the slope is absent in the −1.2 to −0.5 V range and downward from −0.5 V and on, which excludes metallic lead as a possible origin of this slope. The absorption patterns due to surface states as well as the character of their dependencies on potential reported in refs 60 and 61 differ from those observed in Figures 2, 3, and 6. At the same time, it is known[1,21] that, apart from the oxidation film (another phase), the polishing creates a damaged galena surface layer of p-conductivity due to incorporated oxygen (acceptor defects). In the potential region limited by the onsets of the anodic and cathodic decomposition, the potential falls mainly across the space charge region, resulting in changing occupancy and density of these levels. At a cathodic potential bias, these defects dissolve, and a lead-rich layer with donor defects is developed. At a reverse positive potential bias, occupancy of these levels changes. On this basis, the high-wavenumber absorption can be tentatively assigned to the sum absorption of the defects in the surface layer.

According to the electrochemical oxidation mechanism proposed above, the collectorless flotation of galena in deaerated atmosphere at alkaline pH[9,10] can be interpreted as follows. The galena floatability between +0.15 and +0.35 V with the maximum at +0.25 V is due to the formation of the sulfur-rich layer by reaction 1b and crystallization of elemental sulfur by reaction 7 rather than by reactions 1a and 2. The floatability is suppressed by precipitation of $Pb(OH)_2$, which is favored in indifferent electrolytes of higher ionic strengths and for reduced minerals. This may explain, in particular, why the flotation rate for galena ground in a steel mill (in a reducing environment) is lower compared to that of galena ground in a ceramic mill.[9] The flotation is completely canceled when sulfur is oxidized with the formation of PbS_2O_3 by reaction 6b. The shift of the maximum recovery to +0.45 V for the reduced galena in bicarbonate buffer[10] can be due to the specific adsorption of carbonate and formation of lead carbonate, instead of $Pb(OH)_2$.

Conclusions

The FTIR spectra of the galena/solution interface were measured in situ for the first time, allowing one to interpret the indirect data on the anodic oxidation of galena at moderately alkaline pH in a way which does not coincide with the previous interpretations. It is important that not only the vibrational spectra of the surface and interface compounds but also the hole absorption was analyzed, which provided information about the charge-transfer process at the interface. In combination, these data appeared to be sufficient to conclude that at the first step galena is oxidized by reaction 1b, which is followed by reactions 7 and 6a,b. Lead hydroxide is formed by the precipitation mechanism. The yield increases with increasing buffer concentration and degree of galena reduction before the anodic oxidation, which can be explained by increasing the potential drop in the Helmholtz layer.

Acknowledgment. I thank the Russian Foundation for Basic Research (RFBR) for financial support under Grant No. 99-03-32614 and Dr. B. Palsson (Division of Mineral Processing, Lulea University of Technology, Sweden) for calculating ion equilibria and providing the solubility products of the lead compounds.

References and Notes

(1) Richardson, P. E.; Li, Y.-Q.; Yoon, R.-H. *XVIII International Mineral Processing Congress*, May 23−28, 1993, Sidney; Ausralasian Institute of Mining and Metallurgy (AIMM): Parkville, Victoria, Australia, 1993; Vol. 3, pp 757−766.

(2) Nowak, P.; Laajalehto, K.; Kartio, I. *Colloids Surf.* **2000**, *161*, 447.

(3) Woods, R. In *Principles of Mineral Flotation. The Wark Symposium*; Jones M. H., Woodcock, J. T., Eds.; AIMM: Parkville, Victoria, Australia, 1984; pp 91−116.

(4) Becker, U.; Hochella Jr., M. F. *Geochim. Cosmochim. Acta* **1996**, *60*, 2413.

(5) Fletcher, S.; Horne, M. D. *Int. J. Miner. Process.* **1991**, *33*, 145.

(6) Richardson, P. E.; O'Dell, C. S. *J. Electrochem. Soc*. **1985**, *132*, 1350.

(7) Gardner, J. R.; Woods, R. *J. Electroanal. Chem*. **1979**, *100*, 447.

(8) Lekki, J.; Chmielewski, T. *Fizykochem. Probl. Mineralurgii* **1989**, *21*, 127 (in Polish).

(9) Trahar, W. J. In *Principles of Mineral Flotation*; Jones, M. H., Woodcock, J. T., Eds.; AIMM: Parkville, Victoria, Australia, 1984; pp 117−136.

(10) Hayers, R. A.; Ralson, J. *Int. J. Miner. Process*. **1988**, *23*, 55.

(11) Chernyshova, I. V. *J. Phys. Chem. B* **2001**, *105*, 8185.

(12) Ahlberg, E.; Broo, A. E. *Int. J. Miner. Process*. **1991**, *33*, 135.

(13) Buckley, A. N.; Woods, R. *Appl. Surf. Sci.* **1984**, *17*, 401.

(14) Buckley, A. N.; Walker, G. W. In *XVI International Mineral Processing Congress*; Forssberg, K. S. E., Ed.; Elsevier: Amsterdam, 1988; Part A, pp 589−599.

(15) Buckley, A. N.; Kravets, I. M.; Shchukarev, A. V.; Woods, R. *J. Appl. Electrochem*. **1994**, *24*, 513.

(16) Buckly, A. N.; Woods, R. *J. Appl. Electrochem*. **1996**, *26*, 899.

(17) Kartio, I. J.; Laajalehto, K.; Suoninen, E. J.; Buckley, A. N.; Woods, R. *Colloids Surf.* **1998**, *133*, 303.

(18) Schuhmann, D. Flotation. In *Proceedings of the 2nd Latin-American Congress, Concepcion*, Aug 19−23, 1985; Elsevier: Amsterdam, 1988; p 65.

(19) Ndzebet, E.; Schuhmann, D.; Vanel, P. *Electrochim. Acta* **1994**, *39*, 745.

(20) Schuhmann, D. *New J. Chem*. **1993**, *17*, 551.

(21) Peuporte, Th.; Schuhmann, D. *J. Electroanal. Chem*. **1995**, *385*, 9.

(22) Woods, R. *Electrochemistry of Sulfide Mineral Flotation, Lectures*; School of Science, Griffith University: Australia, 2000.

(23) Hsiesh, Y. H.; Huang, C. P. *J. Colloid Interface Sci.* **1989**, *131*, 537.

(24) Kim, B. S.; Hayers, R. A.; Prestige, C. A.; Ralson, J.; Smart, R. St. *Langmuir* **1995**, *11*, 2554.

(25) Wittstock, G.; Kartio, I.; Hirsch, D.; Kunze, S.; Szargan, R. *Langmuir* **1996**, *12*, 5709.
(26) Sun, Z.; Forsling, W.; Rönngren, L.; Sjöberg, S. *Int. J. Miner. Process.* **1991**, *33*, 83.
(27) Sun, Z.; Forsling, W.; Rönngren, L.; Sjöberg, S.; Schindler, P. W. *Colloids Surf.* **1991**, *59*, 243.
(28) Lam-Thi, P. O.; Lamache, M.; Bauer, D. *Electrochim. Acta* **1984**, *29*, 217,
(29) Paul, R. L.; Nicol, M. L.; Diggle, J. W.; Saunders, A. P. *Electrochim. Acta* **1978**, *23*, 625.
(30) Avdokhin V. M.; Abramov, A. A. *Oxidation of Sulfide Minerals in the Ore Processing*; Nedra: Moscow, 1989 (in Russian).
(31) Schuhmmann, D.; Guinard-Baticle, A. M.; Vanel, P.; Talib, A. *J. Electrochem. Soc.* **1987**, *134*, 1128.
(32) Nowak, P.; Laajalehto, K. *Appl. Surf. Sci*. **2000**, *157*, 101.
(33) Chernyshova, I. V.; Andreev, S. I. *Appl. Surf. Sci*. **1997**, *108*, 225.
(34) Turcotte, S. B.; Benner, R. E.; Riley, A. M.; Li, J.; Wadeworth, M. E.; Bodily, D. M. *J. Electroanal. Chem*. **1993**, *347*, 195.
(35) Buckley, A. N.; Woods, R. *J. Electroanal. Chem*. **1994**, *370*, 295.
(36) Christensen, P.; Hammett, A. *Electrochim. Acta* **2000**, *45*, 2443.
(37) Ozanam, F.; da Fonseca, C.; Rao, A. V.; Chazalviel, J.-N. *Appl. Spectrosc*. **1997**, *51*, 519.
(38) Erne, B. H.; Stchakovsky, M.; Ozanam, F.; Chalzaviel, J.-N. *J. Electrochem. Soc*. **1998**, *154*, 447.
(39) Erne, B. H.; Ozanam, F.; Chalzaviel, J.-N. *J. Phys. Chem. B* **2000**, *104*, 11591.
(40) Maroun, F.; Ozanam, F.; Chalzaviel, J.-N. *Surf. Sci.* **1999**, *427*−*428*, 184.
(41) Maroun, F.; Ozanam, F.; Chalzaviel, J.-N. *J. Phys. Chem. B* **1999**, *103*, 5280.
(42) Chernyshova I. V.; Tolstoy V. P. *Appl. Spectrosc*. **1995**, *49*, 665.
(43) Greenler, R. G. *J. Phys. Chem*. **1962**, *66*, 879.
(44) Persson, I.; Persson, P.; Valli, M.; Fozo, S.; Malmensten, B. *Int. J. Miner. Process.* **1991**, *33*, 67.
(45) Leppinen, J. O.; Basilio, C. I.; Yoon, R. H. *Int. J. Miner. Process*. **1989**, *26*, 259.
(46) Mielczarski, J. A.; Mielczarski, E.; Zachwieja, J.; Cases, J. M. *Langmuir* **1995**, *11*, 2787.
(47) Cases, J. M.; de Donato, Ph. *Int. J. Miner. Process.* **1991**, *33*, 49.
(48) Nakamoto, K. *Infrared and Raman Spectra of Inorganic and Coordination Compounds*, 5th ed.; Wiley-Interscience: New York, 1997; Part B.
(49) Kelsall, G. H.; Yin, Q.; Vaughan, D. J.; England, K. E. R.; Brandon, N. P. *J. Electroanal. Chem*. **1999**, *471*, 116.
(50) Morrison, S. R. *The Chemical Physics of Surfaces*, 2nd ed.; Plenum Press: New York, 1990.
(51) Myamlin, V. A.; Pleskov, Y. V. *Electrochemistry of Semiconductors*; Plenum Press: New York, 1967.
(52) Skorchiletti, V. V. *Theoretical Electrochemistry*, 4th ed.; Khimia: Leningrad, 1974 (in Russian).
(53) Latimer, W. M. *The Oxidation States of the elements and Their Potentials in Aqueous Solutions*, 2nd ed.; Prentice Hall Inc.: Englewood Cliffs, NJ, 1952.
(54) Toperi, D.; Tolun, R. *Trans.*—*Inst. Min. Metall., C* **1969**, *78*, C191.
(55) Lurie, Y. Y. *Handbook on Analytical Chemistry*; Mir: Moscow, 1971.
(56) Shchigol, *Zh. Neorg. Khim*. **1963**, *8*, 1361 (in Russian).
(57) Kovalenko, P. N. *Ukr. Khim. Zh*. **1954**, *20*, 549 (in Russian).
(58) Kilthof, I. M.; Stenger, V. A. *Volume Analysis*; Goskhimizdat: Moscow, 1950; Vol. 1, p 325 (in Russian).
(59) Erne, B. H.; Stchakovsky, M.; Ozanam, F.; Chazalviel, J.-N. *J. Electrochem. Soc*. **1998**, *145*, 447.
(60) Rao, A. V.; Chazalviel, J.-N.; Ozanam, F. *J. Appl. Phys*. **1986**, *60*, 696.
(61) Harrick, N. J. *Internal Reflection Spectroscopy*; John Wiley and Sons: New York, 1967.